Available online at www.sciencedirect.com
ScienceDirect
Planetary and Space Science 55 (2007) 755–769
Planetary and Space Science
www.elsevier.com/locate/pss

In search of a new ULF wave index: Comparison of Pc5 power with dynamics of geostationary relativistic electrons

O. Kozyreva[a], V. Pilipenko[b,*], M.J. Engebretson[c], K. Yumoto[d], J. Watermann[e], N. Romanova[a]

[a]*Institute of the Physics of the Earth, Moscow 123995, Russia*
[b]*Space Research Institute, Moscow 117810, Russia*
[c]*Augsburg College, Minneapolis, MN 55454, USA*
[d]*Kyushu University, Fukuoka 812-8581, Japan*
[e]*Danish Meteorological Institute, Copenhagen 2100, Denmark*

Received 4 September 2005; accepted 2 March 2006
Available online 29 November 2006

Abstract

A new ULF wave index, characterizing the turbulent level of the geomagnetic field, has been calculated and applied to the analysis of relativistic electron enhancements during space weather events in March–May 1994 and September 1999. This global wave index has been produced from the INTERMAGNET, MACCS, CPMN, and Greenland dense magnetometer arrays in the northern hemisphere. A similar ULF wave index has been calculated using magnetometer data from geostationary (GOES) and interplanetary (Wind, ACE) satellites. During the periods analyzed several magnetic storms occurred, and several significant increases of relativistic electron flux up to 2–3 orders of magnitude were detected by geostationary monitors. However, these electron enhancements were not directly related to the intensity of magnetic storms. Instead, they correlated well with intervals of elevated ULF wave index, caused by the occurrence of intense Pc5 pulsations in the magnetosphere. This comparison confirmed earlier results showing the importance of magnetospheric ULF turbulence in energizing relativistic electrons. In addition to relativistic electron energization, a wide range of space physics and geophysics studies will benefit from the introduction of the ULF wave index. The ULF index database is freely available via anonymous FTP for all interested researchers for further validation and statistical studies.

Keywords: ULF waves; Electron acceleration; Plasma turbulence; Magnetic storms

1. Introduction: the necessity of a new ULF wave index

The interaction between the solar wind and Earth's magnetosphere is the primary driver of many of the processes occurring in the magnetosphere and ionosphere. This interaction has often been viewed with considerable success using the implicit assumption of quasi-steady and/or laminar plasma flow. However, new conceptions of the magnetospheric plasma dynamics are being developed, in which turbulence plays a fundamental role (Antonova, 2000; Borovsky and Funsten, 2003). Progress in understanding and monitoring these turbulent processes in space physics is hampered by the lack of convenient tools for their characterization.

Various geomagnetic indices (Kp, AE, Dst, SYM-H, PC) and averaged solar wind/IMF parameters quantify the energy supply in certain regions of the solar wind–magnetosphere–ionosphere system, and are used as primary tools in statistical studies of solar–terrestrial relationships. However, these indices characterize the steady-state level of the electrodynamics of the near-Earth environment. The turbulent character of solar wind drivers and the existence of natural MHD waveguides and resonators in the magnetospheric plasma (e.g., the field line Alfven

*Corresponding author.
E-mail addresses: kozyreva@ifz.ru (O. Kozyreva), pilipenk@augsburg.edu (V. Pilipenko), engebret@augsburg.edu (M.J. Engebretson), yumoto@geo.kyushu-u.ac.jp (K. Yumoto), jfw@dmi.dk (J. Watermann), kmosc@mail.ru (N. Romanova).

0032-0633/$ - see front matter © 2006 Elsevier Ltd. All rights reserved.
doi:10.1016/j.pss.2006.03.013

resonator) in the ULF frequency range (~2–10 mHz) ensures a quasi-periodic magnetic field response to forcing at the boundary layers. Therefore, much of the turbulent nature of plasma processes of solar wind–magnetosphere–ionosphere interactions can be monitored with ground-based or space observations in the ULF frequency range. We have attempted to construct a new index, coined a "ULF wave index", characterizing the turbulent character of the energy transfer from the solar wind into the upper atmosphere and the short-scale variability of near-Earth electromagnetic processes. We suppose that a wide range of space physics studies (some of them are listed in the Section 4) will benefit from the introduction of this new index. In this paper we concentrate on just one problem, which is of primary importance for space weather studies, and where the new ULF wave index is vitally necessary—the dynamics of relativistic electrons.

1.1. Magnetospheric turbulence and the energization of relativistic electrons

The appearance at geosynchronous orbit of relativistic electrons following some geomagnetic storms resists definitive explanation in spite of many years of study. These electron events are not merely a curiosity for scientists, but can have disruptive consequences for geosynchronous spacecraft (Wilkinson, 1991). While it has been known that there is a general association between geomagnetic storms and electron enhancements at geosynchronous orbit (Reeves, 1998), the wide variability of the observed response and the puzzling time delay (~1–2 days) between storm main phase and the peak of the response has frustrated the identification of responsible mechanisms and controlling parameters. The observations of Kanekal et al. (1999), Li et al. (1999), and McAdams and Reeves (2001) showed that the enhancements in electron energies (beyond levels expected from conserving adiabatic invariants) at geosynchronous orbit occur rapidly at the onset of a magnetic storm, often within a few hours, but there is also a slower additional acceleration, varying from storm to storm, so that peak fluxes are often seen only after a number of days.

Ultimately, the solar wind is the energy source for geomagnetic storms in general and acceleration of electrons to relativistic energies in particular. However, since the solar wind does not directly contact the electrons in question, some magnetospheric intermediary must more directly provide the energy to the electrons. ULF waves in the Pc5 band have emerged as a possible energy reservoir (Rostoker et al., 1998). This led to proposals for a gradual slow energization of seed electrons of a few hundred keV which are usually supplied by substorms owing to resonant interaction of drifting electrons with MHD oscillations in the Pc5 frequency range (Elkington et al., 1999; Liu et al., 1999; Hudson et al., 2000; Summers and Ma, 2000). This drift-resonance mechanism is in fact a revival of the old idea of a "geosynchrotron" (see references in (Pokhotelov et al., 1999)). More advanced numerical and analytical models provided a description of electron diffusion and acceleration (similar to the quasi-linear theory in plasma physics) upon drift-resonant interaction with low-m (m is the azimuthal wave number) MHD waves (Bahareva and Dmitriev, 2002; Elkington et al., 2003).

Further observations favored the idea of ULF wave-related acceleration of magnetospheric electrons. In a study of the May 1997 storm by Baker et al. (1998) the wave power in the nominal Pc5 band at one of the CANOPUS stations rapidly increased less than 1 h before the appearance of relativistic electrons, prompting the authors to suggest that Pc5 pulsations were an acceleration mechanism for these electrons. The use of one station only is evidently insufficient to validate the role of global ULF wave activity in energizing magnetospheric electrons. There is better observational support for a ULF contribution to the later, slower energization of electrons. In a comprehensive study, O'Brien et al. (2001) performed a superposed epoch analysis to compare storms with and without the appearance of relativistic electrons, using hourly noon-reconstructed electron fluxes (>2 MeV) from GOES and LANL geosynchronous monitors. They showed that elevated Pc5 wave power during the recovery phase appeared to discriminate better than Dst or AE between those storms that do and do not produce relativistic electrons. Similarly, Mathie and Mann (2001) showed that electron events had higher Pc5 power at the mid-latitude SAMNET stations by about an order of magnitude in the recovery phase. Main phase intensity did not appear to be an important indicator of subsequent electron behavior.

For these studies, O'Brien et al. (2001) constructed a wave power index (in this paper named for brevity the B-index) calculated from Fourier spectra in a 2 h sliding window from 11 selected INTERMAGNET stations with L between 3.5 and 7.0. Spectral power from all magnetic vector components was summed up in the 150–600 s band, and the station with the highest power was chosen. However, the B-index needs to be further elaborated to avoid the following drawbacks: (a) usage of the vertical Z component, which is very sensitive to local geoelectric inhomogeneties and cannot be a good indicator of magnetospheric ULF wave intensity; (b) The limited number of stations used, unevenly distributed among MLT sectors; (c) Any LT was considered, so the B-index may be strongly influenced by irregular nightside substorm activity. A similar measure of 1–10 mHz ULF wave activity, but calculated from selected stations from the SAMNET and IMAGE arrays, was used by Mann et al. (2004).

Moreover, the usage of a wave index based on band-integrated wave power only may be insufficient, because this type of index cannot discriminate between irregular wide-band variations and narrow-band waves. For example, a simple measure of the fraction of narrow-band pulsations in observed wave power, the ratio R_G between the wave power in a narrow band (2–10 mHz) and wide

band (0.2–10 mHz), was applied by Posch et al. (2003) to the analysis of ULF dynamics during GEM storms. The ULF activity during the main phase was broad-band (R_G was low), while the ULF activity in the recovery phase was narrow-band in the dawn-to-noon LT sector (R_G was high). Furthermore, very intense irregular variations in the nominal Pc5 frequency band that are observed during the storm main phase are caused by other mechanisms than typical Pc5 pulsations. In particular, their transverse spatial scale is much less than is required for resonance with drifting relativistic electrons (Pilipenko et al., 2001). Thus, a convincing statistical evaluation of possible coupling between ULF activity and relativistic electron dynamics demands a quantitative measure to characterize ULF behavior, comprising both total power and character of the spectra. This measure of ULF wave activity should be taken into account by any adequate model of relativistic electron dynamics, and here we introduce such a measure—a ULF wave index.

2. Construction of a ULF wave index

We derive a ground ULF wave index using the spectral features of ULF power in the Pc5 band averaged over 1 h from a global array of stations in the Northern hemisphere. We use data from the following global magnetometer arrays: INTERMAGNET (www.intermagnet.org), MACCS (space.augsburg.edu/space), CPMN (denji102.geo.kyushu-u.ac.jp/denji/obs), Greenland Coastal Array (www.dmi.dk), as well as data from LRV observatory in Iceland and stations in Arctic Russia (magbase.rssi.ru). The data have been decimated to a common sampling period, 1 min, whenever necessary. A map with station locations is shown in Fig. 1.

The data were inspected for quality, and any daily files with strong interference or large data gaps were purged from the database. The data have been detrended with a cut-off frequency of 0.5 mHz and converted into a geographic (X, Y) coordinate system. For any UT hour, the magnetometer stations in the chosen MLT sector (from LT_1 to LT_2), and in a selected CGM latitude range (from Φ_s to Φ_N) are selected.

For selected stations, the discrete Fourier transform (DFT) spectra of two horizontal components in a desired frequency band are calculated with the use of Filon's formula for calculation of integrals of oscillatory functions (Abramowitz and Stegun, 1998) in a 1 h time window. The signal and background noise spectral contents may be estimated in the following way, similar to Ponomarenko et al. (2002). In a log-linear plot the linear fit $LF(f)$ is applied, which fits the data to a linear model by minimizing the χ^2 σ, in the frequency band from $f_1 = 1$ mHz to $f_2 = 8$ mHz (the Nyquist frequency for a 1-min sampling period is 8.3 mHz). Then, a discrimination line, separating the background noise and signal spectra, is considered as $\log F_B(f) = LF(f) - \sigma$ (as schematically illustrated in Fig. 2). The bump above the discrimination line is considered to be the contribution from a band-limited signal. Alternatively, the background spectrum may be considered as $F_B(f) = LF(f)$ in a log–log plot (not shown), which is a straight line for the "colored-noise" spectrum $\propto f^{-\alpha}$. However, because the frequency range used for the index calculation is relatively narrow, both types of background noise approximation give very similar results.

The frequency range selected for construction of the ULF index is bounded by the lower and upper frequencies f_L and f_H. Noise spectral power in this frequency range is calculated at each jth station as the area beneath the discrimination level (or background spectrum), F_B

$$N_j = \int_{f_L}^{f_H} F_B(f)\mathrm{d}f. \quad (1)$$

Signal spectral power is the area of the bump above the discrimination level, that is

$$S_j = \int_{f_L}^{f_H} \{F(f) - F_B(f)\}\mathrm{d}f. \quad (2)$$

The global ULF wave index is calculated from the band-integrated total power $T_j = S_j + N_j$ at each station by the summation with respect to those N_{st} stations where the power of the signal is above a threshold $K \times \max\{T_j\}$

$$T = \frac{1}{N_{st}} \sum_{j=1,N} T_j. \quad (3)$$

The threshold parameter K may be reasonably chosen between 0.5 and 1.0 (the latter case corresponds to the selection of one station only with maximal amplitude). Similar to (3), the total power of signal and noise components are defined as

$$S = \frac{1}{N_{st}} \sum_{j=1,N} S_j \quad N = \frac{1}{N_{st}} \sum_{j=1,N} N_j. \quad (4)$$

To discriminate between broad-band and narrow-band ULF waves a ratio between signal and total powers is estimated: $R = S/T$. Here R varies in the range 0–1, and when $S = N$, $R = 0.5$. For additional verification of the discrimination technique, we applied an algorithm based on the ratio $R_G = T_{narrow}/T_{wide}$ between the wave power in a narrow band, T_{narrow}, and wide band, T_{wide} (Glassmeier, 1995; Engebretson et al., 1998). However, both approaches provided practically the same results, $R_G \sim R$.

2.1. Additional hourly ULF wave indices

Ground magnetic fluctuations are not always a perfect image of the ULF fluctuations in the magnetosphere. For example, there is a class of ULF waves, called storm-related Pc5 pulsations that occur during the recovery phase of magnetic storms in the dusk and noon sectors of the magnetosphere. These ULF waves are generated by ring current protons via various kinds of drift instabilities (Pilipenko, 1990). Despite their high amplitudes in the magnetosphere, these pulsations are rarely if ever seen on

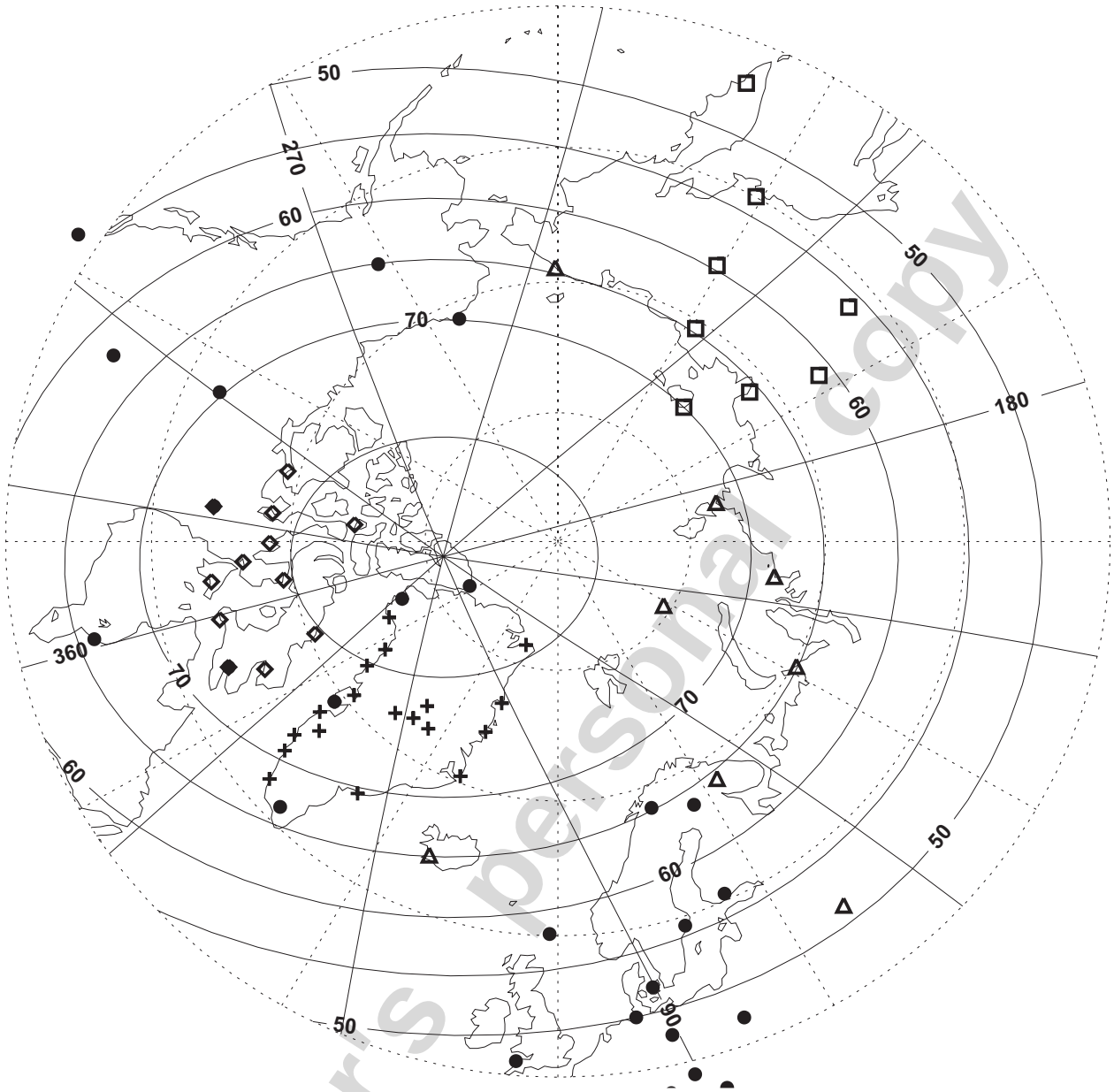

Fig. 1. Map of the ground magnetic stations used for calculation of the global ULF wave index: CPMN (boxes), INTERMAGNET (filled circles), MACCS (diamonds), Greenland coastal chains (crosses), and other stations (triangles).

the ground because their small azimuthal scales (high m-numbers) cause effective screening by the ionosphere. Thus, the ground global index needs to be augmented by a similar index, estimated from data from magnetometers in space. This wave index, coined the GEO ULF index (namely, T_{GEO}, S_{GEO}, and N_{GEO}), is calculated from 1 min 3-component magnetic data from the geostationary GOES spacecraft to quantify the short-term magnetic variability in the region of geosynchronous orbit.

To quantify the short-term IMF variability, an interplanetary ULF index (further named the IMF ULF index, namely, T_{IMF}, S_{IMF}, and N_{IMF}) is estimated using 1-min data from the interplanetary satellites Wind, ACE, and IMP8. The data from these satellites were time-shifted to account for the ballistic propagation (either parallel or using the Weimer et al. (2003) technique) of the solar wind from the satellite location towards the nominal bow shock position. The IMF ULF index is similar but not identical to the hourly value of the IMF component dispersion from OMNI database. For example, for the period 1999–2000 the correlation coefficients r between the IMF ULF index and $\sigma\{B\}$, $\sigma\{B_X\}$, $\sigma\{B_Y\}$, and $\sigma\{B_Z\}$ were 0.4, 0.7, 0.7, 0.78, respectively.

3. Validation of the ULF wave index

To demonstrate the significance of this index for some storm intervals we analyze the variability of the IMF, solar

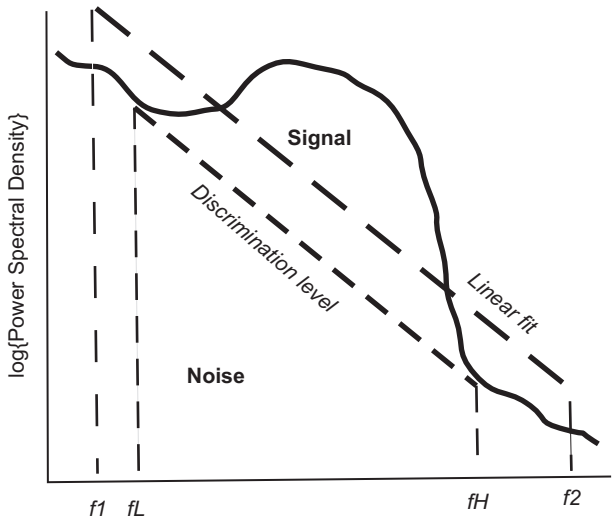

Fig. 2. Schematic plot of the technique for the discrimination of signal and noise from the power spectral density of ULF variations.

wind, and electron radiation near the geosynchronous orbit, together with existing static indices and the ULF wave index. This comparative analysis will elucidate the role of ULF turbulence in the particle response to solar wind forcing and demonstrate the merits and disadvantages of the wave index.

The following parameters have been used for the calculation of the ULF index. The selection of magnetic stations has been made in the MLT sector from $MLT_1 = 03$ to $MLT_2 = 18$, and in the CGM latitude range from $\Phi_S = 60^\circ$ to $\Phi_N = 70^\circ$. The frequency range is from $f_L = 2.0$ mHz to $f_H = 7.0$ mHz, and the discrimination level has been estimated by a linear fit in the frequency interval $f_1 = 1$ mHz to $f_2 = 8$ mHz. The threshold parameter K is set to 1.0, which means that only the station with peak ULF power in this time interval was selected. The data from interplanetary satellites have been time-shifted according to the Weimer propagation model.

Despite many seemingly arbitrarily chosen parameters the output index is rather robust and is not strongly influenced by slight deviations of these parameters from selected values. The extension of the latitudinal selection range beyond 60–70° does not influence the index produced. The peak ULF intensity is always within this range of latitudes, though during large magnetic storms the Pc5 activity extends much further to lower latitudes. The upper band frequency, f_H, has no effect because of the relatively small contribution of high frequencies to the total spectral power. The increase/decrease of the lower band frequency, f_L, causes a subsequent decrease/increase of the level of total power T, but all temporal variations remain very similar. Using a larger number of selected stations for the current ULF power estimate (that is, choosing $K<1$) produces more smoothed and lower values of the global index. The optimal set of parameters can be chosen only after thorough validation of the proposed index by independent researchers.

Using a limited number of stations unevenly distributed along MLT sectors, and the influence of mid-night substorm activity, both inherited by earlier versions of the ULF index, might be expected to produce a bias. This has been examined by the comparison of the new ULF wave index (T_{GR}), calculated for all available stations at any LT, with the earlier B-index of O'Brien et al. (2001) (11 INTERMAGNET stations at any LT) during years 1994–1995. The rank cross-correlation between them is high, $r\sim0.8$ (Fig. 3). This high correlation indicates that increasing the number of stations does not change the basic features of the index. So, for a future ULF index just a limited number of selected stations (~10) should be necessary.

The cross-correlation between new ULF wave indices calculated for 00–24 and 03–18 MLT intervals (not shown) has turned out to be very high, ~0.95, which indicates that irregular ULF activity during night hours provides only a minor contribution to global ULF index.

Thus, the ground ULF wave index based on the calculation of global Pc5 wave power is rather robust, and improvements made have not changed the basic features of its temporal variations. Therefore, all the results obtained with earlier versions of the ULF wave power index (O'Brien et al., 2001; Mathie and Mann, 2001; Mann et al., 2004) remain valid.

3.1. 1994 March–May storms

As an example, we consider the period March–May 1994, namely 03/03 (DOY = 063)—05/17 (DOY = 137). Fig. 4 shows the space weather parameters, space radiation and ULF wave activity during this period as characterized by the Dst index, relativistic (>2 MeV) electron fluxes J_e (count/cm^2/s/sr) at GOES-8, and various ULF indices.

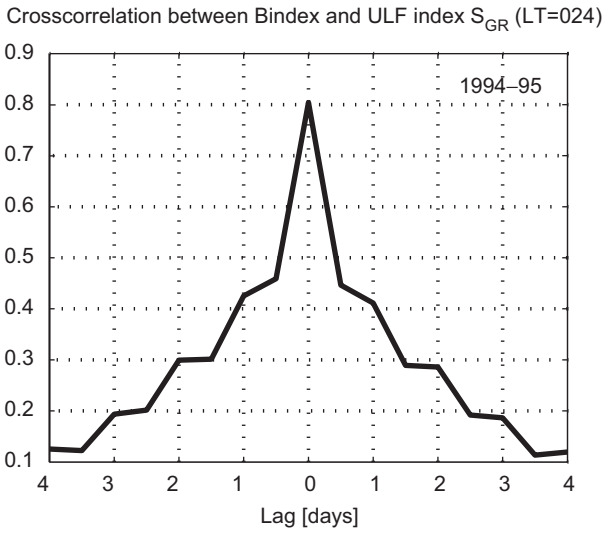

Fig. 3. Cross-correlation function between the ground ULF index S_{GR} (all available world-wide stations) and the earlier B-index of O'Brien et al. (2001) (11 stations) during 1994–1995.

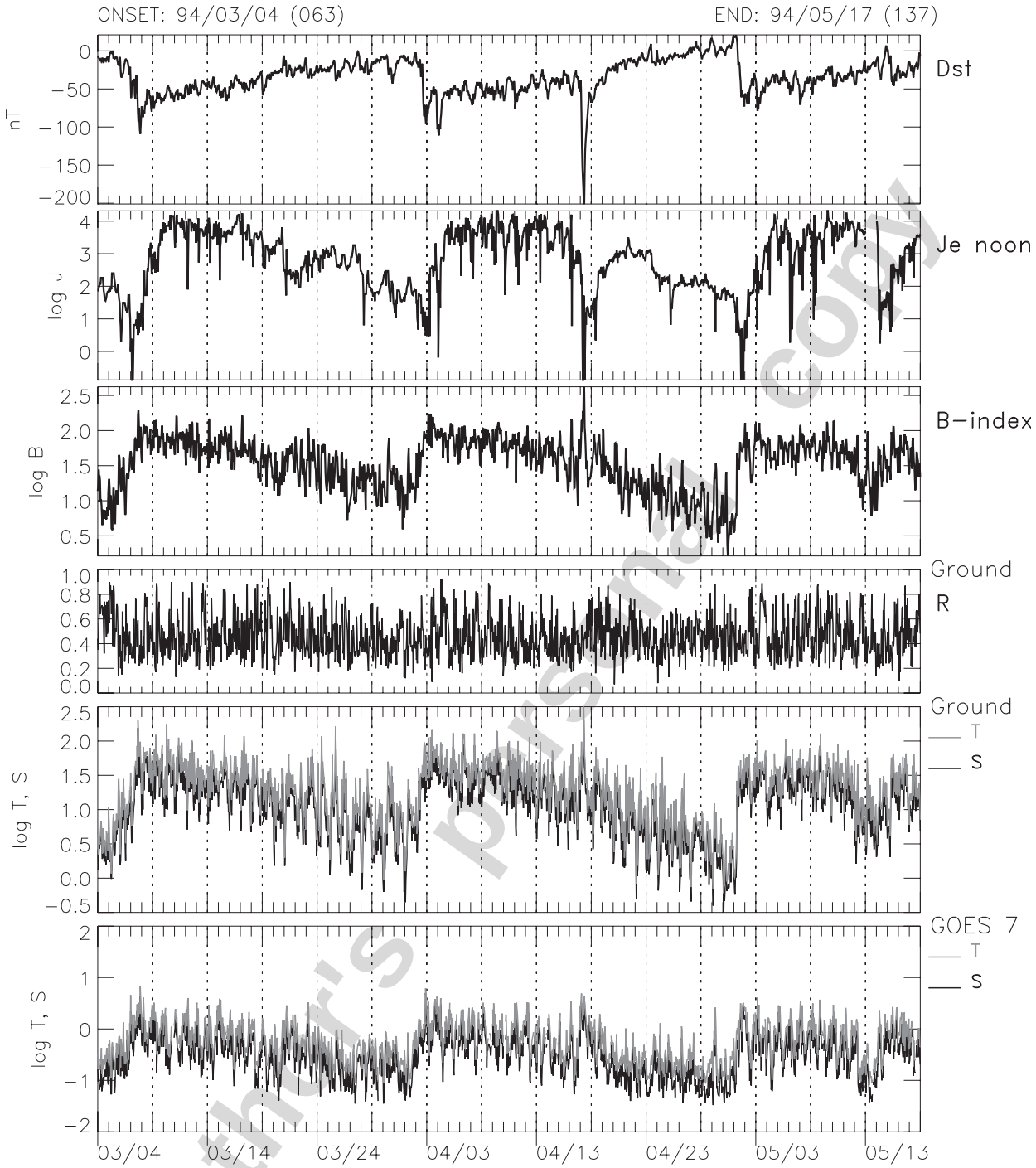

Fig. 4. Comparison of relativistic electron fluxes with magnetic and ULF activity for the period March–April 1994 as characterized by: the Dst index; the GOES-8 noon-reconstructed integral fluxes of electrons >2 MeV; O'Brien's B-index; the ratio $R = S/T$, the ground ULF index (total power T_{GR}, shown in grey, and narrow-band power S_{GR}, shown in black); and the geostationary ULF indices T_{GEO} (grey) and S_{GEO} (black) derived from the Hp component observed by GOES-7.

Solar wind and IMF data from the OMNI-2 database have large data gaps and are not shown.

For this period, hourly noon-reconstructed relativistic electron fluxes J_e at the geosynchronous spacecraft GOES-8 ($\sim$75°W) are available (courtesy of P. O'Brien and G. Reeves), and are shown in the second panel of Fig. 4. The proxy-noon fluxes have no diurnal variations as compared with raw electron data. The fifth panel shows the ULF ground power index, namely $\log_{10} T$, calculated from the global array of ground stations. Some diurnal variations of this global ULF index are caused by the lack of stations in some MLT sectors. The bottom panel shows the GEO ULF index calculated from the magnetometer data from GOES-7 (only the Hp component was available). A surprisingly good overall correspondence can be seen between the time dynamics of the ground ULF index and

the GEO ULF index, keeping in mind that T_{GR} characterizes global wave activity, whereas T_{GEO} responds to local wave activity at a certain longitude.

Comparison with the *B*-index developed by O'Brien et al. (2001), shown in the third panel, indicates a good correspondence between this index and the new ULF index. It should be remembered that the B-index is smoother because of its 2-h averaging window as compared with the 1-h window used for production of the ULF index.

The fraction of the narrow-band component *R* (forth panel in Fig. 4) does not demonstrate consistent results: the irregular variations of $R\sim0.3$–0.8 obscure a temporal pattern. The time variations of the total power index (*T*) and of the narrow-band part of spectrum (*S*) are very similar (fifth panel in Fig. 4).

During this period, several magnetic storms with various intensities occurred, from Dst~-50 nT to Dst~-200 nT, and long-term enhancements of J_e are observed after each storm. However, no association between the storm intensity (Dst) and J_e can be seen. The GOES-8 relativistic electron fluxes demonstrate several enhancements, after each storm, with a peak delay about 1–2 days. But, a sustained intense increase of J_e (above 10^4) is observed after the weak storms, whereas the increase after the strong storm on 04/17 is much shorter and less intense (only up to 10^3). At the same time, the electron behavior matches well the variations of the global ULF index (fifth panel in Fig. 4): after the first two storms this increases much more substantially and for a longer period than after the third storm.

Both the ULF-index and *B*-index correspond well ($r\sim0.7$) to the GEO ULF index calculated from GOES-7 data (Hp component), shown in the bottom panel of Fig. 4.

During the storms in the March–May 1994 period geostationary satellites suffered numerous anomalies due to magnetospheric relativistic electrons ("killer" electrons). Bursts of relativistic electron fluxes produced a swarm of malfunctions onboard the geostationary satellites (Pilipenko et al., 2005). As Fig. 4 shows, the "killer" electron flux has a time delay about 2 days with respect to the ULF wave index, therefore, the ULF wave index could be used as a "precursor" of the risk of geostationary satellite malfunctions during the declining phase of the solar cycle.

3.2. Space weather month: September 1999

In this section, we consider Space Weather Month (September 1999). Fig. 5 shows the space weather parameters, such as the solar wind velocity *V*, plasma density N_p, IMF magnitude *B*, north–south IMF component B_z, and the Dst index, together with the relativistic electron fluxes J_e (>2 MeV) at GOES-10 ($\sim141^\circ$W) during the period from 09/10 (DOY = 253) to 09/30 (DOY = 273). During this interval, a strong magnetic storm occurred on 09/22 (Dst = −164 nT) and 3 weak storms (Dst about −50 nT) occurred on 09/12, 09/16, and 09/27.

The main storm was caused by a shock (solar wind pressure pulse up to 15 nPa), followed by a large interplanetary magnetic cloud with south to north field rotation. The strong IMF *Bz* early in the magnetic cloud drove a major magnetic storm on 09/23. Both strong and weak storms were accompanied by high solar wind streams, enhancements of the solar wind density and IMF magnitude, and negative IMF *Bz* excursions (Fig. 5). The increases of *V* and *Np* were nearly the same during both strong and weak storms, up to 650 km/s and 40/cm^3, correspondingly, but the *Bz* excursion and kinetic pressure were larger for the strong storm.

The main phase of the strong storm on 09/22 is shown in magnetograms of the X component from ground stations in the latitudinal range 60–75° together with 3-component magnetograms from the GOES-10 and ACE (time shifted) satellites (Fig. 6). These plots have been regularly produced for each day to verify the quality of the data used to construct the ULF index.

GOES-10 detected several substantial increases of relativistic electron fluxes (>2 MeV) from $\sim10^2$ to $\sim10^4$ on 09/13 and a gradual increase starting on 09/27. Similar behavior was observed at GOES-8 (not shown), but the overall level of electron fluxes was lower, and the increases were more gradual. The sudden drop to $\sim10^0$ on 09/22, observed 1 day before the storm onset on both GOES satellites, is puzzling. It is not likely to be explained by the adiabatic compression of the magnetosphere, as dropouts during storm commencements, because it is not accompanied by a significant magnetic disturbance (as measured by Dst or ground magnetograms).

A comparison of characteristics of ULF activity with relativistic electron dynamics is given in Fig. 7. Global ground ULF indices, both total power ($\log_{10}T$) and narrow-band power ($\log_{10}S$), demonstrate increases comparable in magnitude on 09/12 and 09/26. From 09/13 to 09/20 the ground ULF wave activity remains elevated. At the same time, the main magnetic storm on 09/22–23 is accompanied by short-lived Pc5 waves only, as revealed by a short-term spike in all ULF indices. This analysis shows, in accordance with previous studies, that a significant increase of relativistic electron flux at the geostationary orbit (up to 2–3 orders of magnitude) is observed not during the main magnetic storm, but during the recovery phases of weak storms. The feature of the latter intervals is a long-term elevated level of the ULF index, caused by the occurrence of very intense Pc5 pulsations.

The GEO ULF index, characterizing the intensity of ULF activity at geostationary orbit (fourth panel in Fig. 7), also shows enhancements during magnetic storms, similar to the ground global ULF-index (correlation coefficient $r\sim0.75$). However, some ULF intensification intervals (e.g., 09/17) are missed by the satellite. During this interval, the global ground ULF index better corresponds to the

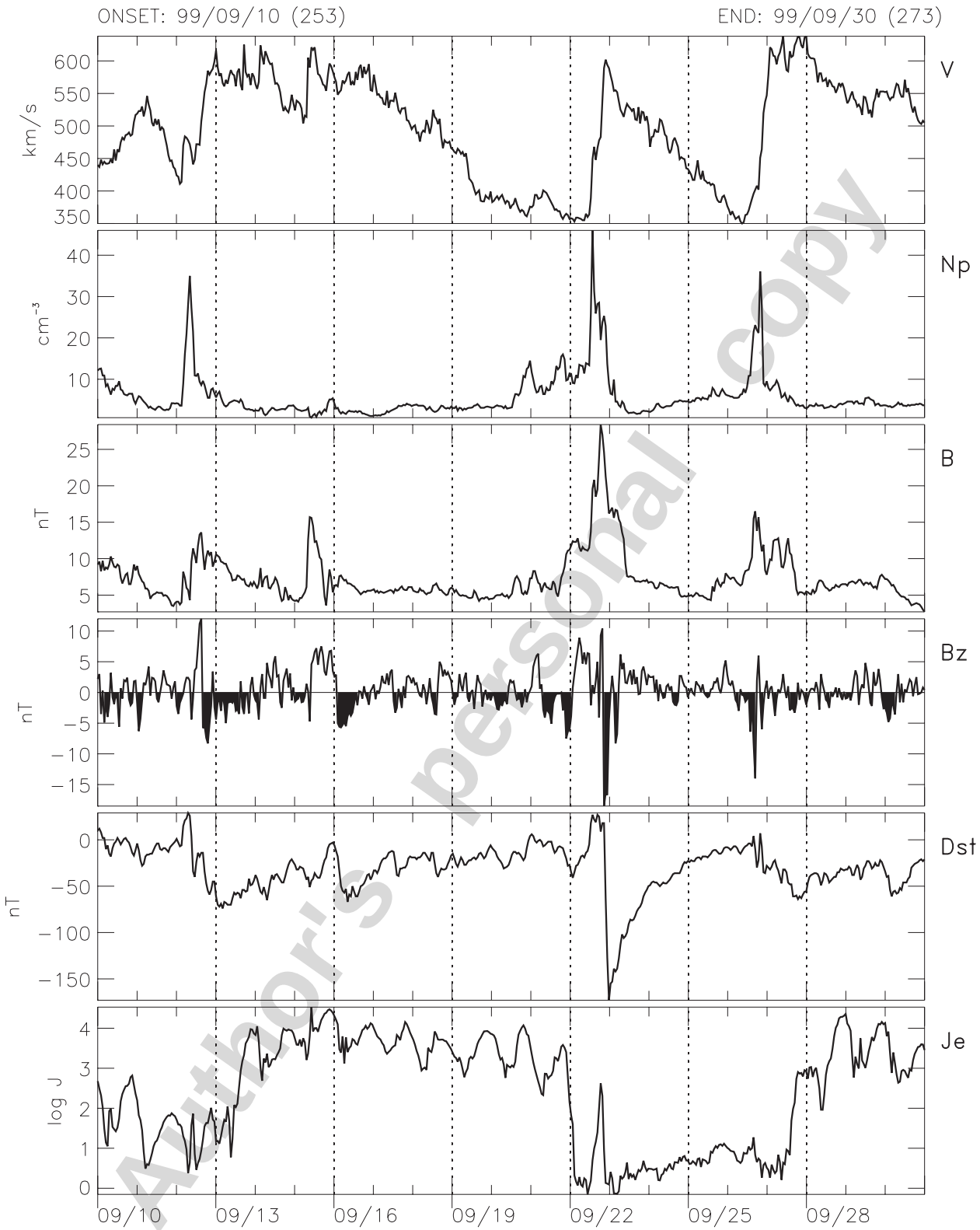

Fig. 5. Space weather parameters during the Space Weather Month period (09/10–09/31): solar wind velocity V; plasma density Np, IMF magnitude B; Bz; Dst; and GOES-10 integral electron (>2 MeV) electron fluxes J_e.

dynamics of relativistic electron fluxes than the local satellite index.

Increases of the ULF index in general coincide with increases of the IMF ULF index calculated from the time-shifted ACE data (third panel in Fig. 7). The correspondence between the ULF activity in the magnetosphere and level of IMF fluctuations in the solar wind upstream of the magnetosphere will be considered elsewhere.

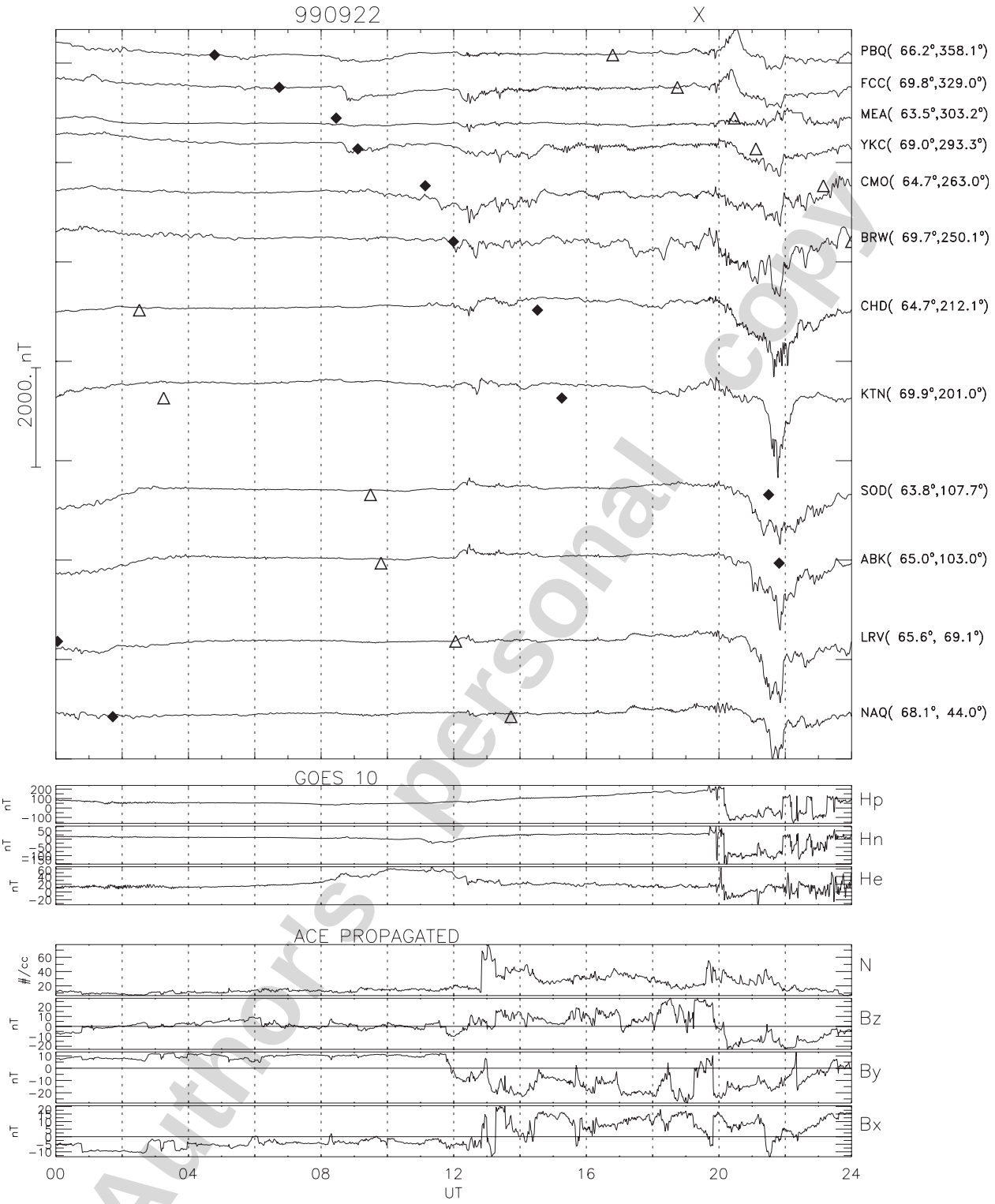

Fig. 6. Magnetograms of the X component from stations in the latitudinal range 60–70° CGM for 1999/09/22 together with 3-component magnetograms from GOES-10 (middle panel) and time shifted ACE data: solar wind density N and 3-component IMF (bottom panel). Local noon (open triangles) and local mid-night (diamonds) for each ground station are indicated. Station codes and CGM coordinates are indicated at the right.

3.3. Statistical analysis of ULF index and relativistic electrons

The ULF wave index would be especially convenient and productive for statistical studies. Here we present some results of its application to the statistical analysis of the relationships between magnetospheric relativistic electrons and ULF wave activity.

The rank cross-correlation function between the daily averaged values of the noon-reconstructed LANL electron

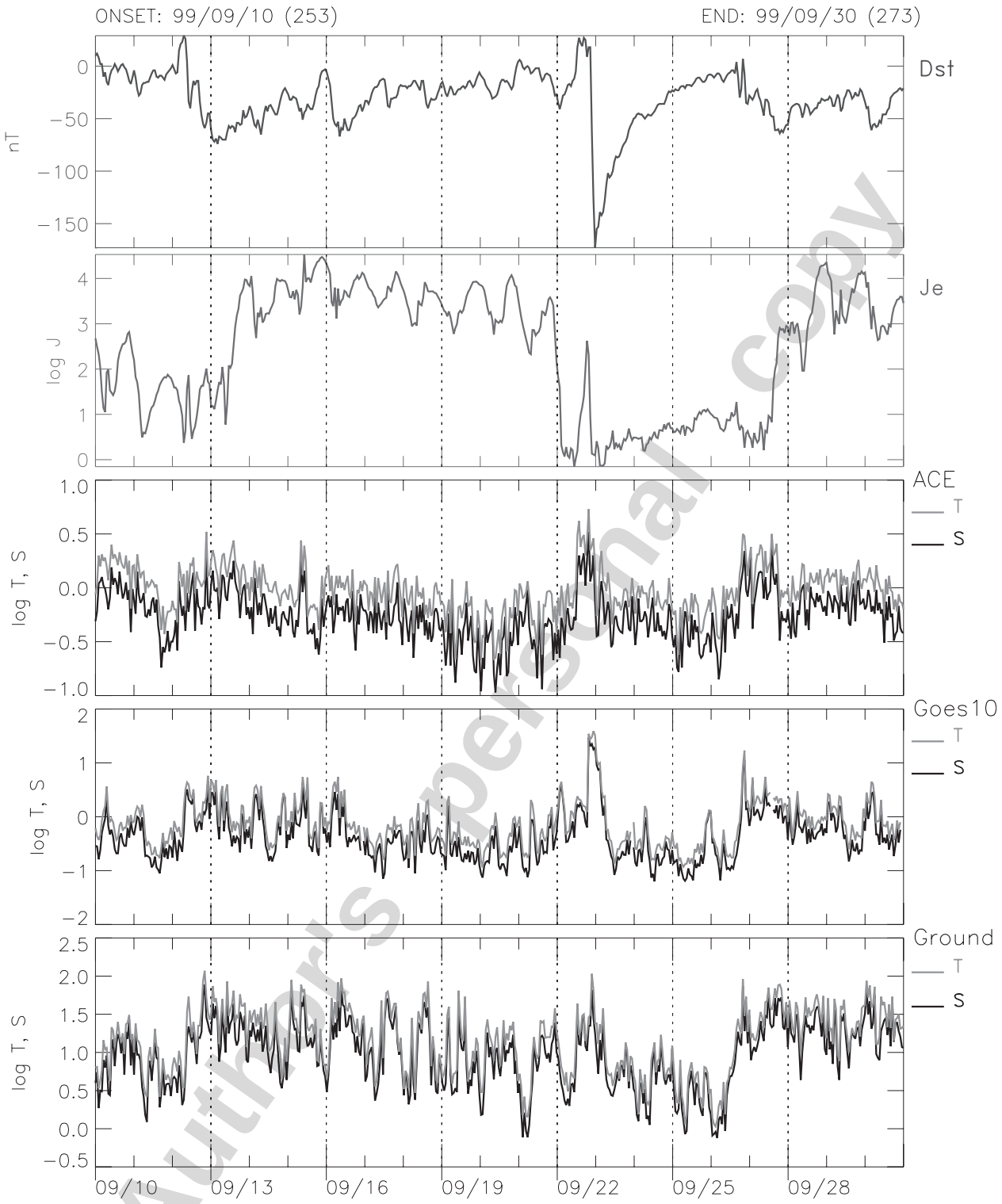

Fig. 7. Comparison of electron fluxes with the storm and ULF wave indices (total power *T*, shown in gray, and narrow-band power *S*, shown in black) during Space Weather Month (09/10–09/31): Dst; GOES-10 integral electron (>2 MeV) electron fluxes J_e; the IMF wave index from propagated ACE data; the GEO ULF wave index derived from 3-component magnetometer data observed by GOES-10; and the global ground ULF index.

(1.7–3.5 MeV) fluxes, solar wind velocity V_{SW}, and various ULF indices for 1994–96 is shown in Fig. 8. This plot demonstrates the well-known fact (e.g., Li et al., 1998; Mann et al., 2004) that the relativistic electron fluxes are highly correlated with V_{SW}.

The offset of the cross-correlation peak indicates that the relativistic electron flux increases about 2 days after enhancement of ULF wave activity. This comparison also shows that the ground ULF index S_{GR} characterizes the electron response somewhat better than the GEO ULF

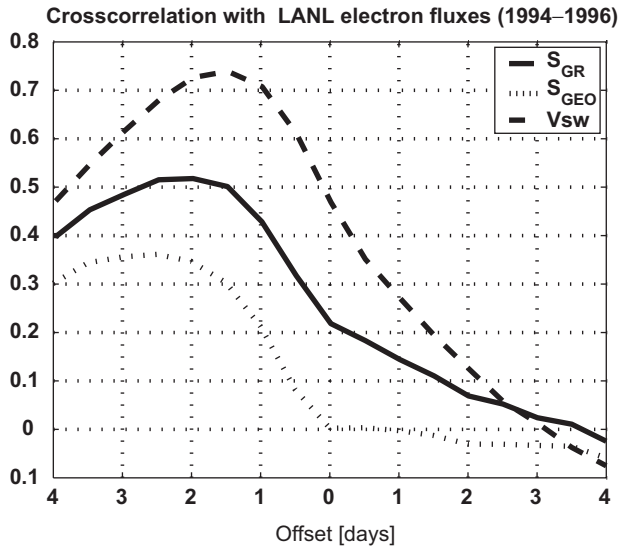

Fig. 8. The cross-correlation between the daily averaged values of the LANL noon-reconstructed electron fluxes (1.7–3.5 MeV) and various ULF indices for 1994–1996.

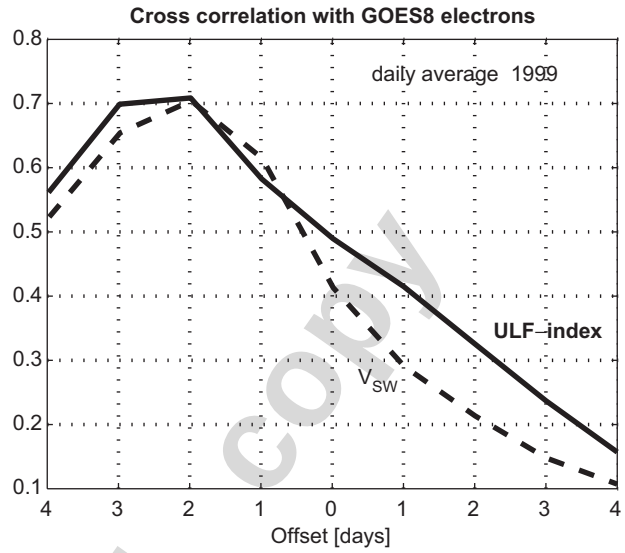

Fig. 9. The cross-correlation of the GOES-8 electron flux (>2 MeV) with the ULF index and solar wind velocity in 1999.

index does. The lower correlation of electrons with the GEO ULF index as compared with the ground ULF index may be caused by the fact that a local GEO monitor could miss many ULF activations that have been detected by a global ground array. Moreover, high-m ULF waves that can be detected in space only probably do not energize the outer radiation belt electrons.

The somewhat different statistical offset (~0.5 days) between the electron response to the solar wind and ULF index is, probably, caused by an offset between the solar wind velocity and ULF activity. Possibly, the ULF wave intensity saturates when solar wind velocity has not reached peak values yet. This question has been discussed by Engebretson et al. (1998) where a possible interpretation was suggested. However, this topic is far beyond the scope of this paper.

Commonly, relativistic GEO electrons correlate with the solar wind velocity better than with any other space weather parameter. However, sometimes the correlation of electron flux with the ULF index is even higher than with the solar wind velocity. For example, Fig. 9 shows the rank cross-correlation function between the GOES-8 electron (>2 MeV) flux and the ULF index S_{GR} and V_{SW} in 1999. The peak value of the cross-correlation function for the ULF index is somewhat higher than that for solar wind velocity. This fact again emphasizes that the ULF index should be taken into account by any adequate space radiation model.

Electron energization and radial diffusion under the influence of ULF wave turbulence are relatively slow processes, so, probably, the current magnitude of the electron flux is determined not by the instantaneous wave intensity, but by a pre-history of wave energy pumping. This consideration is supported by Fig. 10, which shows

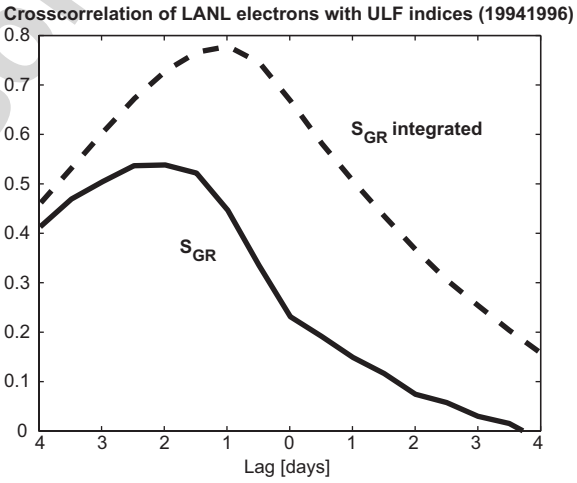

Fig. 10. The cross-correlation of the LANL noon-reconstructed electron flux with the ground ULF index (S_{GR}) and the ground ULF cumulative index (S_{GR}-integrated) in 1994–1996.

the cross-correlation of LANL noon-reconstructed electron (1.7–3.5 MeV) fluxes during 1994–1996 with the cumulative ULF wave index. The cumulative index is the time-integrated index within a characteristic time is τ, as follows:

$$\tilde{I}(t) = \int_{-\infty}^{t} I(t') \exp\left[-(t-t')/\tau\right] \mathrm{d}t'.$$

The cross-correlation coefficient has turned out to be higher for the cumulative index $\tilde{I}$ than for the index I itself. The highest values of r are reached when τ~2 days. Thus, this plot confirms that long-lasting ULF wave activity is more significant for electron dynamics than a short-lived wave burst.

4. Discussion: implications and next steps

In our opinion, the new ULF index better characterizes global Pc5 activity than earlier versions of this index because of better spatial coverage and suppressed contribution of substorm onset to ULF wave power. However, statistical testing has showed that they are in fact very similar ($r\sim0.8$), which may be considered as an additional confirmation of previous results. The newly introduced GEO ULF wave power index and IMF ULF index, together with the more traditional ground ULF index, make it possible to inter-compare the time evolution of low-frequency turbulence in the ionosphere, magnetosphere, and solar wind.

The ULF sub-index *R,* intended to discriminate between broad-band and narrow-band ULF waves, has not demonstrated consistent results. For some stations, *R* grew during a magnetic storm interval indicating that during the main phase the storm-related ULF activity is dominated by wide-band irregular oscillations, whereas during the recovery phase this activity is dominated by narrow-band ULF waves, similar to the observations of Posch et al. (2003). Both *R* and R_G, estimated as the ratio between total power in the 3–7 mHz and 0.2–8.3 mHz bands, gave similar results. However, on a global scale, the irregular variations of *R*, commonly in the range 0.3–0.8, were larger than any storm-related temporal pattern. However, the algorithm implemented here to determine *R* selects the station with peak wave power, but not with highest signal power *S* or highest fraction *R*, so statistically the contribution of the narrow-band component could be obscured. More studies are thus necessary to produce a useful discriminator between narrow-band ULF signals and broad-band noise. The usage of a technique to discriminate between polarized and non-polarized components might also be helpful in the further development of ULF indices.

Thus, the relative ratio *R* derived here between narrow-band and wide-band Pc5 power could not give any confirmative results about the relative importance of wide band noise and narrow band waves for electron acceleration. Nonetheless, the relationships obtained in this paper have demonstrated that even total wave power correlates quite well with the electron variations. This indicates that the energization process is rather diffusive, for which the presence of wave power in a certain frequency range is necessary. This process can be described by the standard plasma physics approximation of weak turbulence—a quasi-linear approximation with stochastic wave phases, as was done by Ukhorskiy et al. (2005). However, in addition to frequency content, it is important that the azimuthal scale of ULF disturbances matches the drift resonance condition $\omega = m\omega_D$. Magnetic activity in the nominal Pc5 band during the main phase and recovery phase has different *m*-scales, not only frequency spectra (Pilipenko et al., 2001), but this feature is not revealed by the current version of the ULF wave index.

Analysis of periods with disturbed space weather in 1994 and 1999 has shown that sustained intense increases of relativistic electron fluxes (up to 2–3 orders) occurred after the weak storms, whereas the increase after the strong storm was much shorter and less intense. The electron behavior matches well the variations of the global ULF-index: after weak storms this index increases much more substantially and for a longer period than after the strong storm. The ULF index shows a significant statistical correlation with the electron dynamics and reveals a time delay of ~2 days between the electron response and ULF wave activity. The observed correspondence between the new ULF wave index and relativistic electron dynamics is consistent with the results of earlier studies by O'Brien et al. (2001) and Mathie and Mann (2001).

During the March–April 1994 storms, geostationary satellites suffered numerous anomalies from "killer" electrons. Because of the ~2 day delay of relativistic electron flux response to the ULF-index, the latter could be used as a "precursor" of the risk of geostationary satellite anomalies. This precursor would be most effective during the declining phase of the solar cycle, when the main menace to spacecraft comes from "killer" electrons, but not from solar protons (Pilipenko et al., 2005). For that, probably, a cumulative ULF-index should be constructed, taking into account an effective acceleration time.

In this paper, we have attempted just to demonstrate the usefulness and ease of use of the ULF wave index for studies of high-energy particle energization in the magnetosphere; we do not claim that the drift resonant interaction with ULF waves is the only mechanism of relativistic electron acceleration (see the reviews of candidate theories of acceleration and transport of radiation belt electrons in Reeves et al. (2003) and Friedel et al. (2002)). Moreover, for a detailed analysis of the acceleration effects it would be desirable to distinguish between temporal variations of electron fluxes caused by adiabatic variations, and variations related to the energization proper.

Though the existing database of the ULF index is already suitable for statistical analysis, in the future we plan to update the technique of index construction. More stations will be included in the analysis, such as the CANOPUS, IMAGE, and new Russian Arctic stations in the northern hemisphere, as well as magnetometer arrays in Antarctica.

4.1. Other possible applications of the ULF wave index

We suppose that in addition to the relativistic electron energization a wide range of space physics studies will benefit from the introduction of this new index. Some of them are listed below:

(1) The degree of coupling of the solar wind flow to the magnetosphere appears to be influenced by the level of

turbulence upstream of the Earth. The magnetosphere indeed is driven more weakly, especially for northward IMF, when the level of solar wind turbulence is low (Borovsky and Funsten, 2003; Goncharova and Pilipenko, 2004). Thus, the magnetosphere behaves in some aspects as a turbulent high-Reynolds-number system, and the presence of turbulence in the flows inside and outside the magnetosphere may have profound effects on its large-scale dynamics through turbulent viscosity and diffusion. Wave indices, characterizing the level of IMF and geomagnetic field turbulence, would be a useful database for the development and statistical verification of this high-Reynolds-number phenomenology of the magnetosphere.

(2) Although there is a modest amount of theoretical and observational evidence supporting the view that elevated level of fluctuations in the solar wind-magnetosphere system favors triggering magnetospheric substorms (Kamide, 2001), this idea has not been thoroughly examined by the space community so far, and it is not used for space weather purposes. Enhanced reconnection and viscous interaction in dayside boundary regions, leading eventually to substorms, most probably are accompanied by an enhanced level of turbulence. Therefore, substorm onset may be preceded by an increased level of ULF power in the region of the dayside boundary layers (Pilipenko et al., 1998). Also, the pre-heating of the nightside plasmasheet plasma owing to the resonant absorption of MHD turbulence may provide necessary conditions for the onset of an explosive instability (the "thermal catastrophe" model of a substorm break-up by Goertz and Smith (1989)). Samson et al. (1992) and Yagova et al. (2000) indicated that ULF fluctuations may play a role in triggering substorm intensifications. Further application of reliable statistical methods for the search for wave precursors of substorms will also benefit from the development of an index quantifying global ULF activity.

(3) A large body of work has demonstrated that it is the solar wind that injects the particles that create the ring current. In this view, it is implicitly assumed that there must be some secondary process that scatters particles from open to closed drift paths. McPherron (1997) suggested that this process is a combination of inherent fluctuations in the solar wind electric fields, waves in the magnetosphere, and inductive electric fields caused by a substorm expansion phase. This process, though being of key importance, is not observable in any existing indices.

(4) Ionospheric studies may also benefit from the introduction of a new ULF wave index. Variations of the ionospheric high latitude electric field may substantially exceed the mean value (Crowley and Hackert, 2001); therefore, the actual Joule heating would be larger than that estimated from the mean time-averaged ionospheric electric field and conductivity. Thus, variability of the electric field, probably measured by the variability of magnetic variations on the ground, should be introduced into climatological models of ionospheric electrodynamics.

(5) Although the proposed ULF wave index is more suited for solar–terrestrial studies, its introduction might be of significant help to the geophysical community developing electromagnetic methods of earthquake prediction. Anomalous ULF noise may occur a few days before strong earthquakes (Fraser-Smith et al., 1990), caused by the crust micro-fracturing at the final stage of the seismic process (Surkov and Pilipenko, 1999). The proposed index will provide the seismic community with an effective tool to distinguish local electromagnetic anomalies in seismo-active regions from global enhancements of ULF wave activity.

5. Conclusion

A new hourly index, analogous to geomagnetic indices, has been derived from ground and satellite magnetometer data. In this paper, we have tried to demonstrate the usefulness of this wave index for the study of relativistic electron energization. However, a wider range of space physics studies, such as substorm physics, solar wind-magnetosphere coupling, etc., may benefit from the introduction of this wave index.

A scientific consortium comprising the Space Physics Laboratory of Augsburg College, Space Environment Research Center of Kyushu University, and Institute of the Physics of the Earth provides the space community with a new ULF wave index. The permanently updating database is freely available via anonymous FTP at the following site for testing and validation: space.augsburg.edu, in the folder: /MACCS/ULF_Index/. Comments and requests for specific intervals or parameters of the ULF index construction are welcomed.

We do not claim that the current index is ready to be adopted as a standard geomagnetic index. Much work is necessary to find and justify the optimal algorithms and parameters. This report is just a step in the elaboration of such a kind of index. Nevertheless, as we have tried to demonstrate in this paper, even the current version of the index may be used to provide reasonable statistical results. Feedback from possible users will facilitate our efforts to improve this index.

Acknowledgments

We acknowledge the provision of data from GOES (NOAA NGDC); the INTERMAGNET project; Leirvogur (LRV, WDC DMI, web.dmi.dk/fsweb/projects/wdcc1); the OMNI-2 database (NASA NSSDC); IMF-propagated data from IGPP UCLA, and noon-reconstructed electron fluxes provided by P. O'Brien and

G. Reeves. Discussions on various aspects of the ULF wave index with P. O'Brien, P. Chi, and I. Mann and the detailed comments of both referees are appreciated. This research was supported by INTAS grant 03-51-5359 (OVK, VAP, JFW), INTAS Young Scientist Fellowship 05-109-4661 (NVR), and NSF grant ATM-0305483 to Augsburg College (MJE).

References

Abramowitz, M., Stegun, I.A., 1998. Handbook of Mathematical Functions with Formulas, Graphs, and Mathematical Tables. Dover, New York, p. 890.

Antonova, E.E., 2000. Large scale magnetospheric turbulence and the topology of magnetospheric currents. Adv. Space Res. 25, 1567.

Bahareva, M.F., Dmitriev, F.F., 2002. Statistical Alfven acceleration of electrons in the outer Earth's magnetosphere. Geomagn. Aeronomy 42, 21.

Baker, D.N., Lepping, R.P., Blake, J.B., Callis, L.B., Rostoker, G., Singer, H.J., Reeves, G.D., 1998. A strong CME-related magnetic cloud interaction with the Earth's magnetosphere: ISTP observations of rapid relativistic electron acceleration on May 15, 1997. Geophys. Res. Lett. 25, 2975.

Borovsky, J.E., Funsten, H.O., 2003. Role of solar wind turbulence in the coupling of the solar wind to the Earth's magnetosphere. J. Geophys. Res. 108, 1246.

Crowley, G., Hackert, C., 2001. Quantification of high latitude electric field variability. Geophys. Res. Lett. 28, 2783.

Elkington, S.R., Hudson, M.K., Chan, A.A., 1999. Acceleration of relativistic electrons via drift-resonant interaction with toroidal-mode Pc5 ULF oscillations. Geophys. Res. Lett. 26, 3273.

Elkington, S.R., Hudson, M.K., Chan, A.A., 2003. Resonant acceleration and diffusion of outer zone electrons in an asymmetric geomagnetic field. J. Geophys. Res. 108, 1116.

Engebretson, M.J., Glassmeier, K.-H., Stellmacher, M., Hughes, W.J., Lühr, H., 1998. The dependence of high-latitude Pc 5 wave power on solar wind velocity and on the phase of high speed solar wind streams. J. Geophys. Res. 103, 26271.

Fraser-Smith, A.C., Bernardi, A., McGill, P.R., Bowen, M.M., Ladd, M.E., Helliwell, R.A., Villard, O.G., 1990. Low-frequency magnetic field measurements near the epicenter of the Ms7.1 Loma Prieta earthquake. Geophys. Res. Lett. 17, 1465.

Friedel, R.H.W., Reeves, G.D., Obara, T., 2002. Relativistic electron dynamics in the inner magnetosphere: a review. J. Atmos. Sol. Terr. Phys. 64, 265.

Glassmeier, K.H., 1995. ULF pulsations. In: Volland, H. (Ed.), Handbook of Atmospheric Electrodynamics, vol. II. CRC Press, Boca Raton, pp. 463–502.

Goertz, C.K., Smith, R.A., 1989. The thermal catastrophe model of substorms. J. Geophys. Res. 94, 6581.

Goncharova, M.Yu., Pilipenko, V.A., 2003. The IMF *Bz* variability—high-latitude magnetic activity index relationship. In: Proceedings of the Conference in memory of Yu. Galperin 3–7 February 2003 Auroral Phenomena and Solar-Terrestrial Relations, Moscow, SCOSTEP, p. 116.

Hudson, M.K., Elkington, S.R., Lyon, J.G., Goodrich, C.C., 2000. Increase in relativistic electron flux in the inner magnetosphere: ULF wave mode structure. Adv. Space Res. 25, 2327.

Kamide, Y., 2001. Interplanetary and magnetospheric electric fields during geomagnetic storms: What is more important, steady-state fields or fluctuating fields? J. Atmos. Sol. Terr. Phys. 63, 413.

Kanekal, S.G., Baker, D.N., Blake, J.B., Klecker, B., Mewaldt, R.A., Mason, G.M., 1999. Magnetospheric response to magnetic cloud (CME) events: relativistic electron observations from SAMPEX and Polar. J. Geophys. Res. 104, 24885.

Li, X., Temerin, M., Baker, D.N., Reeves, G.D., Larson, D., 1998. Quantitative prediction of radiation belt electrons at geosynchronous orbit based on solar wind measurements. Geophys. Res. Lett. 28, 1887.

Li, X., Baker, D.N., Temerin, M., Cayton, T.E., Reeves, G.D., Selesnick, R.S., Blake, J.B., Lu, G., Kanekal, S.G., Singer, H., 1999. Rapid enhancements of relativistic electrons deep in the magnetosphere during the May 15, 1997 magnetic storm. J. Geophys. Res. 104, 4467.

Liu, W.W., Rostoker, G., Baker, D.N., 1999. Internal acceleration of relativistic electrons by large-amplitude ULF pulsations. J. Geophys. Res. 104, 17391.

Mann, I.R., O'Brien, T.P., Milling, D.K., 2004. Correlations between ULF wave power, solar wind speed, and relativistic electron flux in the magnetosphere: solar cycle dependence. J. Atmos. Sol. Terr. Phys. 66, 187.

Mathie, R.A., Mann, I.R., 2001. On the solar wind control of Pc5 ULF pulsation power at mid-latitudes: implications for MeV electron acceleration in the outer radiation belt. J. Geophys. Res. 106, 29783.

McAdams, K.L., Reeves, G.D., 2001. Non-adiabatic response of relativistic radiation belt electrons to GEM magnetic storms. Geophys. Res. Lett. 28 (9), 1879.

McPherron, R.L., 1997. Magnetic storms. In: Tsurutani, B.T., Gonzalez, W.D., Kamide, Y., Arballo, J.K. (Eds.), Magnetic Storms, Geophys. Monograph 98. AGU, Washington, DC, 280pp.

O'Brien, T.P., McPherron, R.L., Sornette, D., Reeves, G.D., Friedel, R., Singer, H.J., 2001. Which magnetic storms produce relativistic electrons at geosynchronous orbit? J. Geophys. Res. 106, 15533.

Pilipenko, V.A., 1990. ULF waves on the ground and in space. J. Atmos. Terr. Phys. 52, 1193.

Pilipenko, V.A., Kozyreva, O., Engebretson, M., Hughes, W.J., Solovyev, S., Yumoto, K., 1998. Coupling between substorms and ULF disturbances in the dayside cusp. In: Proceedings of the International Conference on Substorms-4, Kluwer Academic Publishers, Boston, p. 573.

Pilipenko, V., Kleimenova, N., Kozyreva, O., Engebretson, M., Rasmussen, O., 2001. Global ULF wave activity during the May 15, 1997 magnetic storm. J. Atmos. Sol. Terr. Phys. 63, 489.

Pilipenko, V., Yagova, N., Romanova, N., Allen, J., 2005. Statistical relationships between the satellite anomalies at geostationary orbits and high-energy particles. Adv. Space Res. 37, 1192.

Pokhotelov, O.A., Pilipenko, V.A., Parrot, M., 1999. Strong atmospheric disturbances as a possible origin of inner zone particle diffusion. Ann. Geophysicae. 17, 526.

Ponomarenko, P.V., Fraser, B.J., Menk, F.W., Ables, S.T., Morris, R.J., 2002. Cusp-latitude Pc3 spectra: band-limited and power-law components. Ann. Geophysicae. 20, 1.

Posch, J.L., Engebretson, M.J., Pilipenko, V.A., Hughes, W.J., Russell, C.T., Lanzerotti, L.J., 2003. Characterizing the long-period ULF response to magnetic storms. J. Geophys. Res. 108, 1029.

Reeves, G.D., 1998. Relativistic electrons and magnetic storms: 1992–1995. Geophys. Res. Lett. 25, 1817–1820.

Reeves, G.D., McAdams, K.L., Friedel, R.H.W., O'Brien, T.P., 2003. Acceleration and loss of relativistic electrons during geomagnetic storms. Geophys. Res. Lett. 30, 1529.

Rostoker, G., Skone, S., Baker, D.N., 1998. Relativistic electrons in the magnetosphere. Geophys. Res. Lett. 25, 3701.

Samson, J.C., Wallis, D.D., Hughes, T.J., Creutzberg, F., Ruohoniemi, J.M., Greenwald, R.A., 1992. Substorm intensifications and field line resonances in the nightside magnetosphere. J. Geophys. Res. 97, 8495.

Summers, D., Ma, C.-Y., 2000. Rapid acceleration of electrons in the magnetosphere by fast-mode MHD waves. J. Geophys. Res. 105, 15887–15895.

Surkov, V., Pilipenko, V., 1999. The physics of pre-seismic electromagnetic ULF signals. In: Hayakawa, M. (Ed.), Atmospheric and Ionospheric Electromagnetic Phenomena Associated with Earthquakes. TERRAPUB, Tokyo, pp. 357–370.

Ukhorskiy, A.Y., Takahashi, K., Anderson, B.J., Korth, H., 2005. Impact of toroidal ULF waves on the outer radiation belt electrons. J. Geophys. Res. 110, A10202.

Weimer, D.R., Ober, D.M., Maynard, N.C., Collier, M.R., McComas, D.J., Ness, N.F., Smith, C.W., Watermann, J., 2003. Predicting IMF propagation delay times using the minimum variance technique. J. Geophys. Res. 108, 1026.

Wilkinson, D.C., 1991. NOAA's spacecraft anomaly database and examples of solar activity affecting spacecraft. J. Spacecr. 31, 160.

Yagova, N.V., Pilipenko, V.A., Rodger, A.S., Papitashvili, V.O., Watermann, J.F., 2000. Long period ULF activity at the polar cap preceding substorm. In: Proceedings of the Fifth International Conference on Substorms, St. Peterburg, ESA SP-443, p. 603.